

Division - Soil in Space and Time | Commission - Soil Genesis and Morphology

Alluvial soil formation in the plains of northeastern Brazil

Rafael Cipriano-Silva⁽¹⁾ , Gustavo Souza Valladares⁽²⁾ , Antônio Carlos de Azevedo⁽¹⁾ , Lúcia Helena Cunha dos Anjos⁽³⁾ , Marcos Gervasio Pereira^{(3)*}  and Carlos Roberto Pinheiro Junior⁽³⁾ 

⁽¹⁾ Universidade de São Paulo, Escola Superior de Agricultura Luiz Queiroz, Departamento de Ciência do Solo, Piracicaba, São Paulo, Brasil.

⁽²⁾ Universidade Federal do Piauí, Departamento de Geografia e História, *Campus* Ministro Petrônio Portella, Teresina, Piauí, Brasil.

⁽³⁾ Universidade Federal Rural do Rio de Janeiro, Departamento de Solos, Seropédica, Rio de Janeiro, Brasil.

ABSTRACT: Soils in alluvial plains of the lower course of the Acaraú River, Ceará State, Brazil, are weakly developed and have a complex distribution in the landscape. This study reports the pedogenic characterization of such soils in an effort to understand their formation. Soil pits were opened in four representative sites, profile morphology was described, and soil samples were collected for chemical, physical, mineralogical, and micromorphological analyses. All profiles had weak pedogenic development, as inferred from their morphological characteristics, lack of B horizon, and high silt/clay ratio. Organic carbon and particle size distributions were heterogeneous in Fluvisol, Planosol, and Solonchak, in agreement with their sedimentary nature. Intrinsic characteristics of each profile indicated variations in pedogenic processes related to depositional conditions, which, in turn, were determined by the alluvial nature of sediments and water table dynamics. Consequently, Fluvisols at higher elevations showed reduced pedogenic development. In adjacent areas, Planosols showed pores filled with clay minerals and a texture gradient, indicative of past leaching. Vertisol was identified in small depressions and exhibited intense pedoturbation and high sodium concentration in deep layers. Solonchak had a high degree of hydromorphism, high sodium concentration, and high electrical conductivity. The distinct pedogenesis of alluvial plain soils in Northeastern Brazil is evidenced by their morphological, chemical, and physical properties.

Keywords: clay eluviation, pedogenesis, Inceptisol, pedoturbation.

* Corresponding author:

E-mail: mgervasiopereira01@gmail.com

Received: February 03, 2020

Approved: July 14, 2020

How to cite: Cipriano-Silva R, Valladares GS, Azevedo AC, Anjos LHC, Pereira MG, Pinheiro Junior CR. Alluvial soil formation in the plains of northeastern Brazil. Rev Bras Cienc Solo. 2020;44:e0190110.
<https://doi.org/10.36783/18069657rbc20190110>

Copyright: This is an open-access article distributed under the terms of the Creative Commons Attribution License, which permits unrestricted use, distribution, and reproduction in any medium, provided that the original author and source are credited.



INTRODUCTION

River valleys and plains in Northeastern Brazil form diverse and complex environmental units that may be susceptible to degradation, depending on their land use. Most of these areas are populated by small-scale family farmers that depend on agriculture, livestock, and extractivism to survive. However, some areas should be assigned as permanent preservation areas (Nascimento et al., 2006; Diniz et al., 2008; Mota and Valladares, 2011). Such a scenario creates environmental tension zones. Better knowledge of local soil properties is essential to manage these conflicts efficiently.

Soils of river plains and terraces have good fertility, which, combined with the shallow water table in weakly developed soils, favors crop production with relatively low investment. These favorable conditions are associated with soil geomorphological position, geology, rain seasonality, and fluvial systems (Palmer, 2013). Soil analyses can also contribute to identifying anthropogenic sources of pollutants, particularly herbicides used in agriculture (Gama et al., 2017) and by reconstruction of climate changes recorded in sedimentation patterns caused by alterations in river course and discharge (Damm and Hagedorn, 2010; Celarino and Ladeira, 2017; Bliedtner et al., 2018).

Furthermore, estuarine areas have a rich biodiversity, comprising migratory species that occupy coastal areas. These environments, particularly in Ceará State, are affected by urbanization, deforestation, and shrimp breeding (Nascimento et al., 2006; Mota et al., 2013). Brazilian environmental laws forbid shrimp breeding in mangrove areas but allow the practice in adjacent areas, known locally as *apicum*. Nevertheless, the activity still affects mangroves. The *apicum* is a coastal ecosystem occurring near river deltas in arid or semiarid regions. It is formed by the deposition of sedimentary material, leading to the development of sandbanks in estuaries. This process obstructs mangrove channels and decreases the frequency of tidal flooding, increasing salt concentration in the *apicum*. Thus, the *apicum* is a hypersaline ecosystem in tidal flats that commonly occurs in arid and semiarid coastal regions (Meireles et al., 2007; Albuquerque et al., 2014a,b).

Soil genesis along the Acaraú River basin was driven mainly by climate and sediment deposition. Along its upper course, the river collects sediments from plutonic, metamorphic, and mafic rocks, which are then deposited near the delta. The source material and the semiarid climate, which is unfavorable to soil formation, resulted in the dominance of smectitic clays. Along the plains of the Acaraú River, the most common soils are Luvisols, Leptosols, Cambisols, and Fluvisols, sometimes associated with Planosols. As the river approaches the coastline, Gleysols and Arenosols become frequent. Mangrove and *apicum* areas are strongly affected by water regime and sediment input, which makes them rich in interstratified 1:1 to 2:1 minerals and neoformed illites with high Fe levels (Nascimento et al., 2006; Andrade et al., 2018).

The relative lack of genetically developed soils, the complexity of their distribution across the landscape, and the limited potential for medium- to high-technology agriculture in the study area have discouraged a detailed study of these soils in the past. However, there has been increasing interest in alluvial soils because of their importance to ecological and paleoclimate studies (Buol et al., 2011; Celarino and Ladeira, 2017; Skorupa et al., 2017). Furthermore, their fragility (Mota and Valladares, 2011; Mota et al., 2012), particularly in relation to salinization (Cabral et al., 2019), necessitates an in-depth understanding of their characteristics, as about 70 % of the Acaraú River basin is considered vulnerable (Mota and Valladares, 2011).

Based on the premise that deposition of contrasting sediments has occurred along alluvial plains in the Acaraú River basin, this study aimed to assess the pedogenic alterations and possible pedogenic processes occurring in the soils along the lower course of the Acaraú River.

MATERIALS AND METHODS

Characteristics of the study area

The study was conducted in the lower course of the Acaraú River, northern Ceará State, Brazil (Figure 1). The regional climate is tropical savanna (Aw, Köppen classification system) (Alvares et al., 2013). The annual average temperature is 28.1 °C, evapotranspiration is 1600 mm, relative humidity is 70 %, and precipitation varies from 900 to 1030 mm. Rainfall is unevenly distributed throughout the year, with heavy rains in the first quarter (Diniz et al., 2008). The geology of the region is mainly characterized by igneous and metamorphic rocks derived from the crystalline basement, such as granites, migmatites, gneisses, schists, and quartzites (Sobrinho, 2006). These strata are covered by fluvial and aeolian sediments from the Barreiras Group and the Serra Grande Formation, including conglomeratic sandstones, conglomerates, siltstones, and shales (Sobrinho,

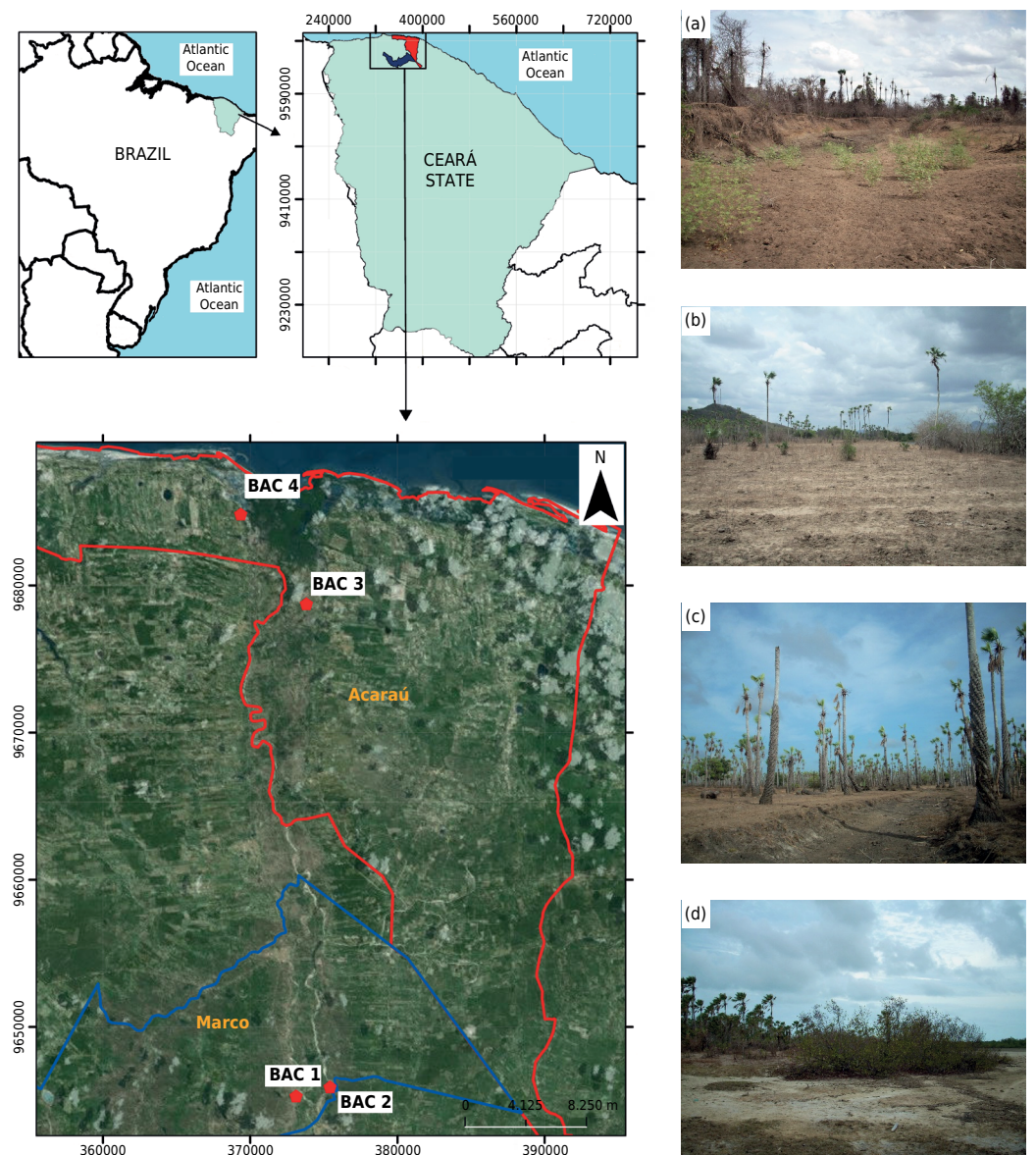


Figure 1. Scheme of location and situation of soil profiles (Zone 24; UTM coordinates). Environment of profile collection BAC1 [Eutric Sodic Fluvisol (Loamic)] (a); environment of profile collection BAC2 [Eutric Fluvisol Planosol (Loamic)] (b); environment of profile collection BAC3 [Sodic Vertisol (Hypereutric)] (c); environment of profile collection BAC4 [Fluvisol Sodic Gleyic Solonchak (Hypersalic, Loamic)] (d). Blue line marks the limit of the municipality of Marco and the red line the limit of Acaraú-CE. Image: Google Earth (2017).

2006; Diniz et al., 2008). Fluvial plains and terraces (0 to 3 % slope) were formed by deposition of clayey and silty sediments. Coastal plains were strongly influenced by the tidal regime and are covered by sandy sediments.

Methods and analyses

Four representative sites in the study region (Figure 1; Table 1) were chosen on the basis of previous studies (Jacomine et al., 1973; Nascimento et al., 2006) and field observations of the physical geography of the area. The soil distribution is intricate, as revealed by the complex map units consisting predominantly of Arenosols (*Neossolos Quartzarênicos*), Gleysols (*Gleissolos*), and Solonchaks (*Gleissolos Sálícos*) in marine plains and Fluvisols (*Neossolos Flúvicos*) and Planosols (*Planossolos*) in fluvial plains and terraces (Nascimento et al., 2006). At each site, the soil profile was described and sampled according to Santos et al. (2015). Samples were air-dried, crushed, and sieved through 2 mm sieves to obtain air-dried fine earth (ADFE) for analysis.

Particle size distribution was determined by the pipette method after dispersion in 0.1 mol L⁻¹ sodium hexametaphosphate (Teixeira et al., 2017). Chemical characterization followed the procedures of Teixeira et al. (2017). Soil pH was determined using a soil/water ratio of 1:2.5 (v/v), electrical conductivity was measured in a saturated soil paste, and total organic carbon (TOC) was quantified by the potassium dichromate (0.167 mol L⁻¹) method. Exchangeable Na⁺, K⁺, and P were extracted with Mehlich-1 solution. Then, K⁺ and Na⁺ levels were determined by flame photometry and P levels by photocolourimetry. Exchangeable Ca²⁺, Mg²⁺, and Al³⁺ were extracted with KCl solution (1 mol L⁻¹) and determined by titration. Potential acidity (H+Al) was determined by 0.5 mol L⁻¹ calcium acetate extraction followed by titration with NaOH. These results were used to calculate the sum of bases ($S = Ca^{2+} + Mg^{2+} + Na^{+} + K^{+}$), effective cation-exchange capacity ($T = S + H + Al$), and exchangeable Na percentage [$ESP = (100 \times Na)/T$].

From each profile, the horizon with the highest degree of pedogenic development was selected for further analysis by X-ray diffraction (XRD), sulfuric acid digestion (Teixeira et al., 2017), and micromorphological examination. The XRD scans were acquired on a MiniFlex II benchtop diffractometer (Rigaku, Tokyo) using Cu K α radiation (30 kV and 15 mA), a Ni filter, a NaI scintillator, and a graphite monochromator. Oriented clay mounts were prepared by treating the clay fraction with citrate-dithionite-bicarbonate (CDB) solution, saturating with K, and heating at 25, 300, and 500 °C. Another aliquot of soil was saturated with Mg and solvated with ethylene glycol at 25 °C before analysis. The K- and Mg-saturated samples were scanned at 0.02° intervals in the 2 θ range of 3 to 50°.

Table 1. General information and classification regarding soil profiles of the lower course of the Acaraú River (Ceará State, Brazil)

Profile	Current vegetation	Drainage	Situation/elevation	Classification	
				WRB	SiBCS
BAC1	Carnaúbas (<i>Copernicia prunifera</i>) and bush-shrubby	Imperfectly drained	River island/25 m	Eutric Sodic Fluvisol (Loamic)	<i>Neossolo Flúvico Sódico sálico</i>
BAC2	Carnaúbas (<i>Copernicia prunifera</i>) and bush-shrubby	Imperfectly drained	Alluvial terrace/23 m	Eutric Fluvisol Planosol (Loamic)	<i>Planossolo Háptico Eutrófico solódico</i>
BAC3	Carnaúbas (<i>Copernicia prunifera</i>) associated with natural pastures	Imperfectly drained	River plain/7 m	Sodic Vertisol (Hypereutric)	<i>Vertissolo Hidromórfico Sódico salino</i>
BAC4	Halophytes plant species as grasses and bush-shrubby	Poorly drained	Fluvial-marine plain/5 m	Fluvisol Sodic Gleyic Solonchak (Hypersalic, Loamic, Ochric)	<i>Gleissolo Sálico Sódico típico</i>

WRB: World Reference Base for Soil Resources (IUSS Working Group WRB, 2015); SiBCS: Brazilian System of Soil Classification (Santos et al., 2018).

For determination of the K_i and K_r indices, soil samples were digested in 1:1 (v/v) sulfuric acid (H_2SO_4) solution in water, brought to the boiling point, cooled to room temperature, and filtered. Ferric (Fe_2O_3), titanium (TiO_2), and aluminum (Al_2O_3) oxides were determined by UV-visible spectrophotometry of the filtered solution. The residue was considered as silica (SiO_2) (Teixeira et al., 2017). Then, K_i and K_r were calculated by the following formulae: $K_i = (SiO_2/Al_2O_3) \times 1.7$ and $K_r = (SiO_2/0.6)/[(Al_2O_3/1.02) + (Fe_2O_3/1.60)]$.

Prior to micromorphological analysis, undisturbed soil samples were pretreated with acetone to remove water and impregnated with a mixture of polyester resin, styrene monomer, and fluorescent pigment under vacuum using methyl ethyl ketone peroxide as polymerization catalyst (Castro and Cooper, 2019). After curing, 30 μm thick sections were mounted on glass slides and examined under a Zeiss petrographic microscope equipped with polarizers. Soil specimens were described using the terminology proposed by Bullock et al. (1985).

Soils were classified according to the World Reference Base (IUSS Working Group WRB, 2015) and the Brazilian Soil Classification System (SiBCS) (Santos et al., 2018).

RESULTS

Soil morphology

The dominant hue of Fluvisol (BAC1), Planosol (BAC2), and Vertisol (BAC3) was 10YR, i.e., a brownish color, with values of 3 to 6 and chromas of 1 to 4 (Table 2). Solonchak showed more yellowish hues (2.5Y and 5Y), with colors becoming more neutral with depth. Variegated colors and/or mottles were observed in all profiles, reflecting restricted drainage conditions.

The structure of Vertisol and Planosol was strong, dominated by prismatic and blocky aggregates but also containing cuneiform and parallelepiped blocks. Fluvisol and Solonchak exhibited a massive structure in subsurface horizons. Slickenside surfaces were abundant in Vertisol and were presented around aggregates in Fluvisol and Planosol.

As a result of the alluvial nature of the parent material, there was great variability in textural classes both with depth and between soil profiles; an exception was Vertisol, which showed a predominance of clay up to a depth of 0.80 m.

Physical attributes

There was no clearly discernible pattern of the particle size distribution (Table 3). In Planosol and Fluvisol profiles, the fine sand fraction predominated over the coarse sand fraction, with Planosol having the highest fine sand values. For Vertisol, there was no major difference between fractions, whereas, for Solonchak, there was a predominance of the coarse sand fraction.

All profiles had high silt contents. Some samples from Fluvisol and Planosol had higher silt than clay contents, affording silt/clay ratios greater than 1.0. Clay content increased markedly with depth in Planosol. High-activity clay was identified in all profiles in the concentration range of 48.5 to 82.5 $cmol_c\ kg^{-1}$ of clay. Only Planosol showed a regular pattern of coarse sand/fine sand ratio, without variation in depth. This parameter varied greatly in Vertisol, from 1.3 in the Cvng horizon to 64.1 in the 2Cn horizon.

Chemical attributes

Soil pH values ranged from strongly acidic (5.2) to moderately alkaline (8.3); however, most horizons were moderately acidic (pH 5.5 to 6.5) (Table 4). Because pH values were somewhat high, exchangeable Al^{3+} was mostly absent, except in some Fluvisol

Table 2. Morphological properties of soil profiles of lower course of the Acaraú River (Ceará State, Brazil)

Hor	Layer	Munsell Color		Structure	Slickensides	Textural class
		Matrix	Mottle			
m						
<i>Eutric Sodic Fluvisol (Loamic) - Neossolo Flúvico Sódico sálico</i>						
A	0.00-0.16	10YR 4/3	10YR 6/8	mo, me, pr	-	Sandy loam
CA	0.16-0.38	10YR 3/3	-	massive	-	Clay loam
Cnz1	0.38-0.92	10YR 4/2	-	massive	-	Clay loam
Cnz2	0.92-1.32	10YR 4/2	-	massive	-	Clay loam
2Cnz	1.32-1.55	2.5YR 4/2	2.5Y 5/6	massive	-	Sandy clay loam
3Cvn	1.55-1.75 ⁺	10YR 4/1	10YR 6/6	massive	com, wk	Clay loam
<i>Eutric Fluvisol Planosol (Loamic) - Planossolo Háplico Eutrófico solódico</i>						
A	0.00-0.20	10YR 3/4	-	st/ mo, f, ab	-	Sandy loam
2A	0.20-0.33	10YR 4/4	-	st, me, pr	-	Clay loam
2E	0.33-0.50	10YR 5/3	-	simple grain	-	Sand
2EB	0.50-0.60	10YR 5/4	10YR 6/8	mo, f, ab	-	Sandy loam
2Bt1	0.60-0.71	Var. 10YR 5/3 and 10YR 3/3	-	st, me/co, pr	-	Silt clay loam
2Bt2	0.71-0.98	Var. 10YR 5/3 and 10YR 4/3	-	st, me/co, pr	-	Clay loam
2Btvnz	0.98-1.40 ⁺	10YR 4/3	-	st, me/co, pr	com, wk	Silt clay loam
<i>Sodic Vertisol (Hypereutric) - Vertissolo Hidromórfico Sódico salino</i>						
Apnz	0.00-0.25	10YR 3/2	-	st, co, pr and ab	-	Clay
CA	0.25-0.47	10YR 3/3	-	st, co, we and pa	com, mo	Clay
Cvng	0.47-0.80	10YR 5/2	-	st, co, we and pa	abu, st	Clay
2Cn	0.80-1.20 ⁺	Var. 2.5Y 6/2 and 7.5YR 6/8	-	simple grain	-	Sand
<i>Fluvisol Sodic Gleyic Solonchak (Hypersalic, Loamic, Ochric) - Gleissolo Sálico Sódico típico</i>						
Agnz	0.00-0.08	Var. 5YR 4/4 and 5YR 3/4	-	wk, f, gr	-	Loamy sand
Cgnz1	0.08-0.32	2.5Y 5/2	5YR 4/4	massive	-	Sandy loam
Cgnz2	0.32-0.50	5Y 4/1	5YR 4/4	massive	-	Sandy clay loam
2Cgnz	0.50-0.72	N4/	5YR 4/4	massive	-	Clay loam
3Cgnz	0.72-0.80	N4/	5YR 4/4	massive	-	Sandy loam
4Cgnz	0.80-1.10 ⁺	N2/	-	massive	-	Loamy sand

Var: Variegated; wk: weak; mo: moderate; st: strong; vf: very fine; f: fine; me: medium; co: coarse; ab: angular blocky; gr: granular; we: wedge; pr: prismatic; pa: parallelepiped; com: common; abu: abundant.

and Planosol horizons, which contained up to $0.4 \text{ cmol}_c \text{ kg}^{-1}$ of Al^{3+} , even at $\text{pH} > 5.5$. Overall, Ca^{2+} and Mg^{2+} levels were high and, in some cases, Mg^{2+} was present in higher amounts than Ca^{2+} , possibly as a result of marine influence. The Na^+ levels were also high, mainly in Vertisol, Fluvisol, and Solonchak, reaching ESP values of 41 %. High ESP and electrical conductivity (EC), associated with a pH lower than 8.0, are indicative of salinization processes in Solonchak, Vertisol, and even in Fluvisol, whose pH was close to 8.0 in some horizons (except in 3Cvn, which had a pH of 8.3). These findings are characteristic of the so-called saline sodic soils ($\text{EC} \geq 4 \text{ dS m}^{-1}$, $\text{ESP} \geq 15 \%$, and $\text{pH} < 8.5$).

Phosphorous content ranged from 0.1 to 15.5 mg kg^{-1} ; however, the highest values were associated with more basic horizons, suggesting that the use of acid extraction (Mehlich-1)

Table 3. Physical properties of soil profiles localized in lower course of the Acaraú River (Ceará State, Brazil)

Hor	Sand			Silt	Clay	Coarse sand/ Fine sand	Silt/Clay	CEC clay
	Total	Coarse	Fine					
g kg ⁻¹								
cmol _c kg ⁻¹								
<i>Eutric Sodic Fluvisol (Loamic) - Neossolo Flúvico Sódico sálico</i>								
A	622	236	386	199	179	0.6	1.1	n.d.
CA	320	109	211	328	353	0.5	0.9	63.5
Cnz1	372	143	229	291	337	0.6	0.9	63.2
Cnz2	359	137	222	343	298	0.6	1.2	73.8
2Cnz	494	268	226	275	231	1.2	1.2	71.0
3Cvn	321	64	257	395	285	0.2	1.4	82.5
<i>Eutric Fluvisol Planosol (Loamic) - Planossolo Háplico Eutrófico solódico</i>								
A	649	55	594	214	138	0.1	1.6	n.d.
2A	389	36	353	237	375	0.1	0.6	n.d.
2E	904	190	714	43	54	0.3	0.8	n.d.
2EB	693	29	664	183	125	0.0	1.5	n.d.
2Bt1	144	7	137	548	309	0.1	1.8	72.8
2Bt2	210	10	200	514	277	0.1	1.9	71.8
2Btvnz	151	19	132	463	387	0.1	1.2	66.7
<i>Sodic Vertisol (Hypereutric) - Vertissolo Hidromórfico Sódico salino</i>								
Apnz	172	84	88	295	534	1.0	0.6	n.d.
CA	155	79	76	315	531	1.0	0.6	48.6
Cvng	250	139	111	312	439	1.3	0.7	48.5
2Cn	977	962	15	3	20	64.1	0.2	n.d.
<i>Fluvisol Sodic Gleyic Solonchak (Hypersalic, Loamic, Ochric) - Gleissolo Sálico Sódico típico</i>								
Agnz	798	536	262	122	80	2.0	1.5	n.d.
Cgnz1	634	487	147	194	173	3.3	1.1	60.1
Cgnz2	521	398	123	215	265	3.2	0.8	62.6
2Cgnz	226	98	128	480	295	0.8	1.6	49.2
3Cgnz	716	544	172	134	151	3.2	0.9	59.6
4Cgnz	836	619	217	94	70	2.9	1.3	n.d.

Hor: horizon; n.d.: not determined. Particle size distribution determined according to Teixeira et al. (2017). CEC clay: cation exchangeable capacity clay (clay activity), coarse sand/fine sand, and silt/clay calculated according to Santos et al. (2018).

might have led to the overestimation of P levels. All profiles had high cation-exchange capacity, sum of bases, and base saturation. Base saturation was very close to 100 %, mostly as a result of the high Na⁺ levels.

The TOC content was low, ranging from 0.5 to 7.5 g kg⁻¹. In Vertisol, TOC content decreased with depth, but in other soils, the distribution was erratic. The SiO₂ contents quantified by sulfuric acid attack ranged from 118 to 230 g kg⁻¹ (Table 5). The Al₂O₃ and Fe₂O₃ levels were low in most samples, yielding Ki and Kr values greater than 3.20 and 2.20, respectively. The highest values of pedogenic oxides, except for TiO₂, were observed in the 2Btvnz horizon of Planosol, and the lowest (for all oxides) were found in the Cgnz2 horizon of Solonchak.

Soil mineralogy

Peak shape and intensity varied greatly between soil profiles, although the XRD patterns of clay fractions revealed similar mineral assemblages (Figure 2). The phyllosilicates

Table 4. Chemical attributes of soil profiles localized in lower course of the Acaraú River (Ceará State, Brazil)

Hor	pH(H ₂ O)	cmol _c kg ⁻¹					%		S	T	ESP	V	P	TOC	EC
		Ca ²⁺	Mg ²⁺	Al ³⁺	Na ⁺	K ⁺	H+Al								
<i>Eutric Sodic Fluvisol (Loamic) - Neossolo Flúvico Sódico sálico</i>															
A	5.9	4.2	5.2	0.2	0.3	0.1	1.4	9.8	11.2	3	88	7.2	4.2	0.4	
CA	6.4	8.6	9.9	0.0	2.2	0.1	1.6	20.8	22.4	10	93	2.9	4.2	0.5	
Cnz1	6.8	6.3	9.1	0.0	5.3	0.1	0.5	20.8	21.3	25	98	11.4	3.7	9.8	
Cnz2	8.0	6.2	7.3	0.0	8.4	0.1	0.0	22.0	22.0	38	100	8.9	2.6	7.2	
2Cnz	7.9	4.3	5.8	0.0	5.9	0.1	0.3	16.1	16.4	36	98	15.5	1.6	4.8	
3Cvn	8.3	7.1	7.1	0.0	9.2	0.0	0.0	23.5	23.5	39	100	7.0	2.5	0.2	
<i>Eutric Fluvic Planosol (Loamic) - Planossolo Háplico Eutrófico solódico</i>															
A	6.1	4.4	3.1	0.0	0.0	0.2	1.5	7.7	9.2	1	84	5.4	5.0	0.6	
2A	5.4	6.7	5.7	0.4	0.1	0.0	2.0	12.6	14.6	1	86	6.1	3.3	0.2	
2E	6.1	1.3	1.4	0.0	0.0	0.0	0.5	2.8	3.3	1	85	1.8	0.8	0.2	
2EB	5.4	4.2	3.4	0.2	0.1	0.1	1.1	7.8	8.9	1	88	4.4	1.4	0.1	
2Bt1	5.8	11.1	8.6	0.3	0.2	0.1	2.4	20.1	22.5	1	89	11.9	4.7	0.1	
2Bt2	6.1	9.5	7.9	0.3	0.3	0.1	2.1	17.8	19.9	1	89	8.5	3.7	0.1	
2Btvnz	6.1	11.6	9.9	0.0	1.7	0.1	2.5	23.3	25.8	7	90	8.2	4.8	5.2	
<i>Sodic Vertisol (Hypereutric) - Vertissolo Hidromórfico Sódico salino</i>															
Apnz	5.2	8.7	8.8	0.0	6.4	0.2	2.1	24.2	26.3	24	92	1.4	7.5	4.1	
CA	5.9	5.4	10.0	0.0	8.7	0.3	1.5	24.3	25.8	34	94	1.0	5.0	4.8	
Cvng	7.0	4.6	8.2	0.0	7.3	0.3	0.9	20.4	21.3	34	96	0.9	3.3	1.7	
2Cn	7.3	0.5	2.1	0.0	0.2	0.0	0.5	2.8	3.3	6	85	0.1	0.5	0.2	
<i>Fluvic Sodic Gleyic Solonchak (Hypersalic, Loamic, Ochric) - Gleissolo Sálico Sódico típico</i>															
Agnz	5.7	2.7	0.7	0.0	1.5	0.8	0.7	5.7	6.4	23	89	2.1	6.8	178.6	
Cgnz1	6.0	1.2	2.8	0.0	3.9	2.0	0.6	9.8	10.4	37	94	4.0	3.0	68.2	
Cgnz2	5.3	1.5	4.5	0.0	6.8	2.6	1.3	15.3	16.6	41	92	2.5	4.3	57.4	
2Cgnz	5.2	1.6	4.1	0.0	5.5	2.2	1.1	13.4	14.5	38	92	3.1	4.8	65.8	
3Cgnz	6.1	1.1	3.0	0.0	2.9	1.4	0.6	8.4	9.0	33	93	3.7	3.8	98.7	
4Cgnz	6.1	1.2	1.7	0.0	1.5	0.4	0.7	4.8	5.5	27	87	2.3	5.1	79.0	

Hor: horizon; pH in water at a ratio of soil:solution equal to 1:2.5; S: sum of exchangeable bases; T: CEC at pH 7.0; ESP: exchangeable sodium percentage [(Na/T)×100]; V = (S/T) × 100; TOC = total organic carbon; EC: electric conductivity. All chemical attributes were determined and calculate according to Teixeira et al. (2017).

Table 5. Pedogenetic oxides, Ki, Kr, and Al₂O₃/Fe₂O₃ ratio of some horizons in the soil profiles localized in lower course of the Acaraú River (Ceará State, Brazil)

Profile	Horizon	g kg ⁻¹					Ki	Kr	Al ₂ O ₃ /Fe ₂ O ₃
		SiO ₂	Al ₂ O ₃	Fe ₂ O ₃	TiO ₂				
Fluvisol	3Cvn	175	83	63	7.4	3.58	2.41	2.07	
Planosol	2Bt2	179	92	62	8.1	3.31	2.30	2.33	
	2Btvnz	230	122	74	8.0	3.20	2.31	2.59	
Vertisol	Cvng	221	115	64	8.3	3.27	2.41	2.82	
Solonchak	Cgnz2	118	58	50	3.9	3.46	2.23	1.82	

Ki = (SiO₂/Al₂O₃) × 1.7; Kr = (SiO₂/0.6)/[(Al₂O₃/1.02)+(Fe₂O₃/1.60)]. Determined and calculate according to Teixeira et al. (2017).

in the clay fraction of all samples were mainly illite (peaks at 1.00, 0.50, and 0.33 nm, with little variation between horizons) and kaolinite (peaks at 0.71 and 0.35 nm that disappeared with heating at 500 °C), as oxides were eliminated by CDB treatment. The low intensity of the illite peak at 0.50 nm may indicate a high Fe content (Andrade et al.,

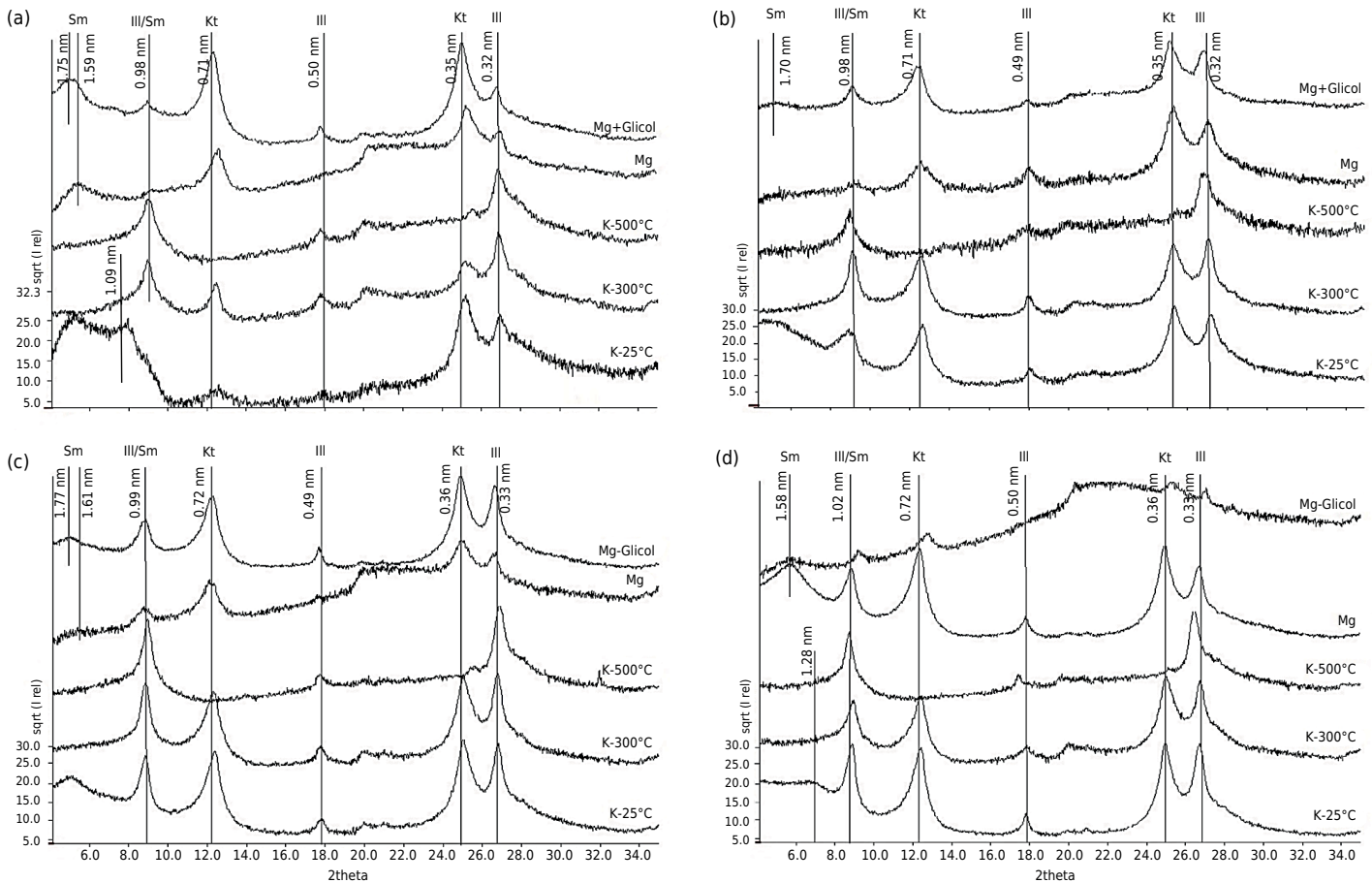


Figure 2. X-ray diffractograms of clay fraction in the horizons or layers in the soil profiles located in the lower course of the Acaraú River (Ceará State, Brazil). (a) horizon 3Cvn (Fluvisol); (b) horizon 2Btvnz (Planosol); (c) horizon Cvn (Vertisol); (d) Horizon Cgnz2 (Solonchak). Sm: smectite; Ill: illite; Kt: kaolinite.

2014). The presence of smectite is indicated by the absence of peak migration from 1.5 to 1.8 nm with Mg + glycol solvation and peak collapse at 1.0 with K saturation in samples treated at 300 and 500 °C. More detailed studies are needed to confirm the occurrence of expansive 2:1 phyllosilicates.

The full width at half maximum was more associated with the degree of crystallinity than with particle size, as analyses were performed using the clay fraction only. Kaolinite did not differ in crystallinity among samples, suggesting that soils were neoformed locally or brought by the river from sites with similar genesis. Also, kaolinite peaks showed no signs of asymmetry, suggesting that this mineral did not share the interstratified particles.

Soil micromorphology

In general, the composition of coarse materials was similar in the studied profiles, with a predominance of quartz followed by feldspar, both of which have subhedral and subangular grain surfaces that are typical of less weathered environments (Table 6). Only the 2Btvnz horizon of Planosol was found to be well sorted; all other horizons were poorly sorted. Fine materials were basically composed of clay minerals and had a yellowish to brownish color associated with the presence of iron oxides (goethite) (Bullock et al., 1985; Kovda and Mermut, 2010). Many birefringent fabric patterns were observed in the studied profiles, including pore-striated fabric in the Cvng horizon of Vertisol and stipple-speckled fabric in Solonchak, findings that may be associated with environments not subjected to contraction and expansion forces. The main types of pores observed were channels, fissures, cavities, and chambers, in different proportions.

Table 6. Micromorphological description of selected horizons in soil profiles localized in lower course of the Acaraú River (Ceará State, Brazil)

Coarse material	Fine material	Microstructure	Pores	Pedological features
Eutric Sodic Fluvisol (Loamic) - Neossolo Flúvico Sódico sálico; 3Cvn (1.55-1.75 m)				
Compose 30 % of the groundmass. Poorly selected, containing quartz (55 %), quartzite (5 %), feldspar (30 %), and other minerals (10 %). Subhedral grains (~90 %). Smooth sub-angular sub-elongated and subspherical.	50 % of groundmass, grayish brow, compose of clays as kaolinite. Stipple-speckled b-factory (40 %). Presence of areas with undifferentiated b-factory.	Angular blocky peds with porphyric distribution. Peds weakly developed, accommodated and with irregular surface, smooth near grains.	Compose 20 %, of which: 10 % are channels, 30 % fissures, 25 % cavities, and 35 % chambers.	Internal hypo-coating of aggregate and in the pores. Few areas with a coating of grains and aggregate, composed of iron oxides and clay. Nodules (1 %) typical, composed of iron and manganese and, or, quartz grains.
Eutric Fluvic Planosol (Loamic) - Planossolo Háptico Eutrófico solódico; 2Btvnz (0.98-1.40 m)				
Compose 40 % of the groundmass. Well-selected and containing quartz (60 %), feldspar (30 %) and other minerals (10 %). Subhedral (60 %) and anedral (40 %) grains. Smooth sub-angular spherical and sub-spherical (~80 %).	30 % of groundmass, olive-yellow, compose of clays as kaolinite and iron oxides (goethite). Predominance of stipple-speckled b-factory.	Sub-angular blocky peds with porphyric distribution. Peds moderately (80 %) and weakly (20 %) developed, partially accommodated and with an irregular surface.	Compose 30 % of which: 35 % are channels, 30 % fissures, 20 % cavities and 15 % chambers.	Internal hypo-coating in the pores. Coating of pores, composed of iron oxides and clay. Pore filling with adherent materials, dense complete (80 %) and incomplete (20 %). Nodules (1 %) typical, composed of iron and manganese and, or quartz grains. Excrement features.
Sodic Vertisol (Hypereutric) - Vertissolo Hidromórfico Sódico salino; Cvng (0.47-0.80 m)				
Compose 20 % of the groundmass. Poorly selected, containing quartz (45 %), quartzite (5 %), feldspar (30 %) and other minerals (10 %). Subhedral grains (~90 %). Smooth sub-angular sub-spherical (70 %).	50 % of groundmass, light yellowish-brown, composed of clays as kaolinite and smectite. Stipple-speckled (70 %), pore-striated and grain-striated (30 %) b-factory.	Angular blocky peds with porphyric distribution. Peds strongly developed, accommodated and with a predominance of smooth rounded and sub-angular surface.	Compose 30 % of which: 65 % are fissures; 20 % chambers, cavities and channels sum 15 %.	Hypo-coating of aggregate and in the pores. Few areas with a coating of grains and aggregate, composed of iron oxides and clay. Nodules (2 %) typical, composed of iron and quartz grains, in the decomposition stage.
Fluvic Sodic Gleyic Solonchak (Hypersalic, Loamic, Ochric) - Gleissolo Sálico Sódico típico; Cgnz2 (0.32-0.50 m)				
Compose 50 % of the groundmass. Poorly selected, containing quartz (70 %), quartzite (10 %), feldspar (15 %) and other minerals (5 %). Subhedral grains. Smooth subangular spherical and sub-spherical (80 %); and smooth angular subspherical (20 %)	35 % of groundmass, grayish brown, composed of clays as kaolinite. Stipple-speckled (80 %) and mosaic-speckled (20 %) b-factory.	Massive structure, with few areas weakly developed (15 %). Porphyric distribution.	Compose 15 % of which: 40 % are channels, and 60 % cavities.	Predominance of internal hypo-coating in the pores by compounds of iron amorphous. Nodules (1 %) typical, composed of iron and quartz grains.

Only the Solonchak (Cgnz2) did not show an aggregated microstructure (massive) or pores from root activity. A well-developed, angular blocky structure was observed in Vertisol (Cvng) and a weak-developed structure in Fluvisol (3Cvn), whereas Planosol (2Btvnz) exhibited a moderately-developed, subangular blocky structure. Pedological features such as iron and manganese nodules and iron hypocoatings were observed in all profiles (Figures 3, 4, 5, and 6). Additionally, pore and aggregate coating were observed in Fluvisol, Vertisol, and, with greater intensity, in Planosol.

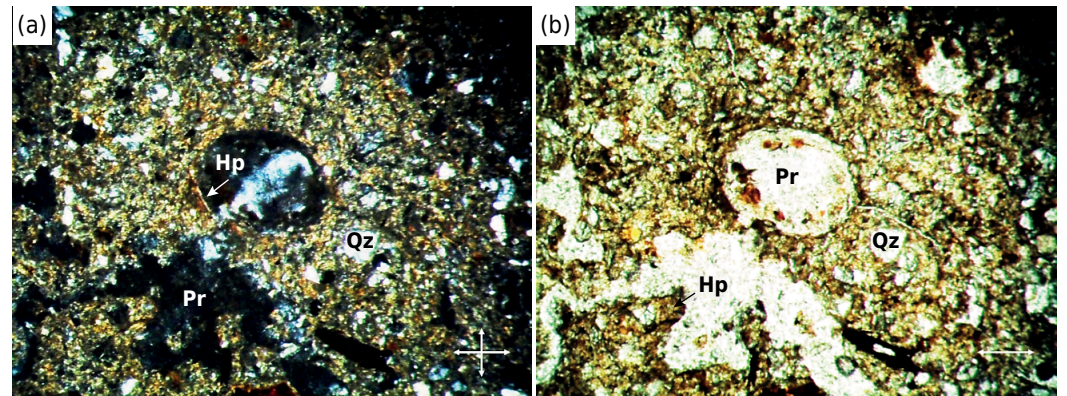


Figure 3. Photomicrographs images of 3Cvn layer in the Fluvisol [(a): cross-polarized light; (b): natural light]. Presence of irregular pores (Pr); quartz (Qz) in the coarse material and features of hypo-coating (Hp).

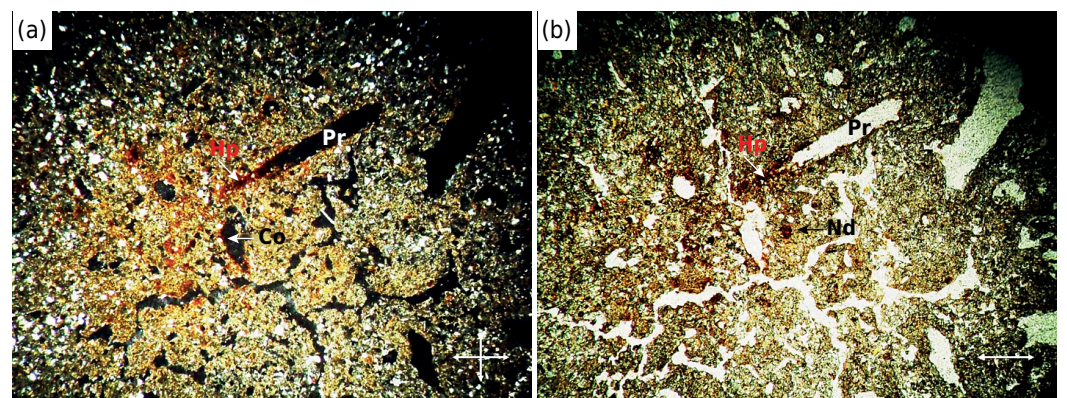


Figure 4. Photomicrographs images of 2Btvnz horizon in the Planosol profile [(a): cross-polarized light; (b): natural light]. Presence of pores (Pr) and features of coating (Co), hypo-coating (Hp), and typical nodule (nd).

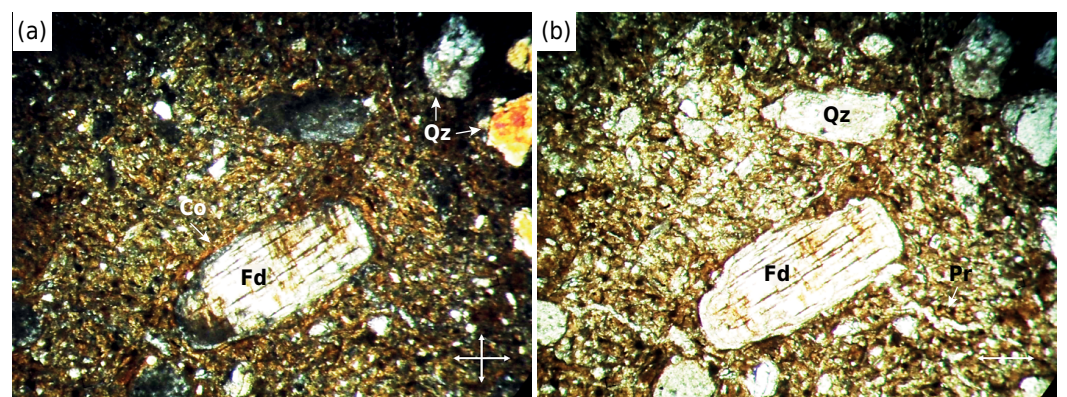


Figure 5. Photomicrographs images of Cvng layer in the Vertisol profile [(a): cross-polarized light; (b): natural light]. The presence of quartz (Qz) and feldspar grains (Fd) composed the coarse material and features of coating (Co).

DISCUSSION

Morphological and physical attributes

Soil profiles differed greatly in depth, horizon/layer thickness, and fluvio-marine depositional environments, leading to differences in chemical and morphological features. Hydromorphic features, on the other hand, were common to all profiles.

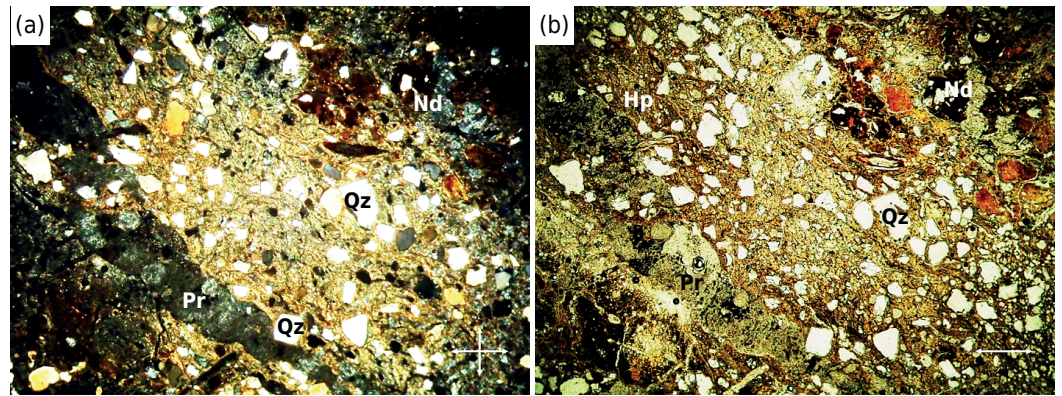


Figure 6. Photomicrographs images of Cgnz2 layer in the Solonchak profile [(a): cross-polarized light; (b): natural light]. Presence of quartz (Qz) and nodule (Nd) in the groundmass. Features of hypo-coating (Hp) probably iron and, or, manganese in the pores (Pr).

Solonchak morphology suggested a great degree of hydromorphism, in agreement with the results of Albuquerque et al. (2014a). The occurrence of gleying can be inferred from the neutral colors with values below 4 and abundant mottles at depth. In Solonchak and Fluvisol, the massive structure in subsurface horizons was likely the result of water saturation at some period of the year.

A vertic character was assigned in deep horizons to Planosol (2Btvnz, 0.98-1.40 m) and Fluvisol (3Cvn, 1.55-1.75⁺ m) (Santos et al., 2018) as there were features that indicated both the expansion and contraction of the soil matrix. A planic B horizon was identified in Planosol by the abrupt textural change. There was an increase in clay content at the subsurface and variegated colors with hue 10YR associated with chroma 3, indicating imperfect drainage (Santos et al., 2018).

Particle size analysis showed textural variability between horizons in a profile and between profiles, attributed to the deposition of parent materials. Because of the proximity to the shore, the area might have been influenced by past transgressive events that contributed to the input of coarse, mainly quartz-rich sand. This type of sand may also have been deposited by wind during dune migration (Meireles et al., 2007; Albuquerque et al., 2014a). The presence of silt and fine sand fractions in Fluvisol and Planosol might be related to the low hydric potential of the lower course of the Acaraú River, leading to the transport and deposition of particles smaller than sand in such areas (which are more distant from the sea).

Silt/clay ratio and silt content are diagnostic attributes used to infer the degree of sediment weathering. The results suggest that the analyzed soils have a low level of development. For soils developed from sediments, a high silt/clay ratio and a low coarse sand/fine sand ratio are indications of a fluvic character. Such a pattern was observed in all profiles, especially in Fluvisol.

Chemical attributes

The chemical attributes of the studied profiles are the result of processes that typically occur in fluvio-marine environments, such as high evapotranspiration rates and water table fluctuations, which promote salt accumulation (Buol et al., 2011). Thus, it is common that soils in semiarid climates and in sedimentary basins have large quantities of easily weatherable minerals and of elements in the soil solution such as K^+ , Ca^{2+} , Mg^{2+} , and Na^+ (Nascimento et al., 2006; Bétard et al., 2009).

The low TOC levels are a consequence of the scarcity of vegetation and plant biomass, and the high oxidation rate that results from the high temperatures. These findings agree with those of Parahyba et al. (2010), who studied the soils of the Brazilian Semiarid

region. The depth-varying distribution of carbon is the main characteristic of Fluvisol, not observed in other soils.

Solonchak had the highest values of EC and ESP, corroborating previous studies conducted under similar conditions (Ferreira et al., 2010; Albuquerque et al., 2014a). The results highlight the role of the marine environment and *apicum* as sources of Na^+ , as well as Ca^{2+} and Mg^{2+} , in soil. Added to the excess evapotranspiration in relation to precipitation, these conditions explain the hypersalinity of soil (Albuquerque et al., 2014a).

Pedogenic oxides, mineralogy, micromorphology, and genesis

The high Ki index (>3.0) and morphological characteristics of evaluated soils indicated a low degree of pedogenesis. The presence of 2:1 phyllosilicates, confirmed by XRD, and the low Fe_2O_3 levels explain the high Ki indices. Low Fe_2O_3 content, in turn, was associated with system deferritization (Melo et al., 2001) from impeded drainage, particularly in Solonchak. The clay mineralogy is in agreement with the dry climate, characterized by high evapotranspiration and the interception of the water table by the topographic surface, reducing leaching to a minimum (Andrade et al., 2014; Albuquerque et al., 2014a; Cabral et al., 2019).

Fluvisol probably had the largest degree of interstratification (Figure 2a), evidenced by the broad band at 1.1-1.8 nm (2θ range of 8° to about 5°). The mineral easily collapsed to 1.0 nm with K saturation at 300°C , with a peak larger than that of the main kaolinite peak at 0.7 nm (2θ of about 12°) (Barnhisel and Bertsch, 1989). Although relative intensities are reported, comparison of peak heights within a sample relates to the number of atomic plans diffracted and, therefore, is indirectly associated with the amount of the phase in the sample. The interstratified mineral peak splits into two with Mg saturation at 25°C , and shows a single band when saturated with Mg + glycol (1.8 nm), suggesting an interstratified illite/smectite. For this hypothesis to be tested, a specific protocol of sample preparation, scanning, and data processing would have to be carried out. The lack of exchangeable Al^{3+} , resulting mainly from the high pH, implies small Al^{3+} activity and unsuitable condition to the deposition of Al-hydroxy into the 2:1 interlayers and the formation of hydroxy-interlayered smectite (HIS), which would be an even more complex mineral (Barnhisel and Bertsch, 1989; Sartor and Azevedo, 2014). This explains the high cation-exchange capacity of Fluvisol (Table 4) despite its low clay content (300 g kg^{-1}) (Table 3). The Fluvisol profile was located farther from the estuary of the Acaraú River and at a higher elevation (25 m) than the other profiles. It had the lowest pedogenic development of all profiles in terms of morphology, Ki index, 2:1 phyllosilicate peak intensity, and clay activity.

Micromorphological results supported this interpretation, as primary minerals were slightly weathered and poorly selected, with angular shapes in the 3Cvn horizon. In this profile, the pattern of orientation was stipple-speckled because of the irregular distribution of fine material (clay minerals). The weak microaggregate development was directly related to the low degree of pedogenic development of Fluvisol, as evidenced by its morphological description. The presence of fissures, and at their intersection the presence of chamber-type pores, result from the great variation of soil volume by expansion and contraction, due to the 2:1 minerals (Kovda and Mermut, 2010). Furthermore, these characteristics favor pedoturbation, which destroys clay coatings and explains their scarcity (Parahyba et al., 2010). Hypocoatings were identified on some pores, possibly of iron and manganese because of the brownish colors. The coatings were darker than the matrix background, indicating temporary reducing conditions. Similar features were observed by Celarino and Ladeira (2017) in the Bg horizon of a Fluvic Gleysol.

Because of the complexity of the river course, particularly in medium and lower sections, the occurrence of alluvial plains is common. In alluvial plains, the river channel widens and generates intermittent river channels during the flooding season (Diniz et al., 2011).

Alternation of dry and rainy seasons might have led to erosion, transport, and deposition of sediments in the area where Fluvisol was developing and in the fluvial island nearby. Therefore, the area is still unstable, strongly influenced by the fluvial regime, and linked to landscape evolution (Eze et al., 2016).

The Planosol was located near the Fluvisol area, in a fluvial terrace close to the Acaraú River. The geomorphic surface seemed to be older and more stable, as it was slightly more elevated than that of the Fluvisol. It was the only profile that did not show a sodic character (ESP >15 %).

Planosol (Figure 2b) XRD spectra showed a wide band from 1.1 to 1.8 nm (2θ range of 7.5 to 5.0°; K saturation at 25 °C), which was more intense than the illite peak at 1.0 nm. After K saturation at 300 °C, the band disappeared, and the intensity of the illite peak at 1.0 nm increased. The smectite band was also visible, more defined with Mg + glycol solvation (1.7 nm), but still small. This result agrees with the high clay activity of Planosol (especially in Bt1 and Bt2). A fully functional smectite phase has a greater cation-exchange capacity than an illite/smectite interstratified mineral.

Micromorphological analysis of the B horizon of Planosol revealed coarse material dominated by better sorted, finer-grained quartz than that of Fluvisol. These features, as well as the higher proportions of fine sand and silt, suggest lower transport energy during the fluvial processes that brought these materials (Celarino and Ladeira, 2017). The matrix background had stipple-speckled orientation and concentrated zones of low crystallinity Fe oxides near pores, implying segregation and rapid precipitation. In the field, such zones appear as small mottles and are the result of fluctuations in the water table and seasonal soil saturation, as is common in Planosols (van Ranst et al., 2011). Nodules of both sharp and diffuse contrasts were identified by the release of iron from the matrix background (Pineiro Junior et al., 2019). Although the variation of TOC with depth was also evident in Planosol, which is typical of fluvial deposition (fluvic character), the greater pedogenic development of Planosol compared to Fluvisol was confirmed by morphological features. The presence of clay coatings, although in small amounts, indicated leaching contributed to the texture gradient (Pineiro Junior et al., 2019). Scarcity of such coatings may also be the result of their destruction by changes in soil mass volume, caused by the high activity and expansivity of clay minerals (Kovda and Mermut, 2010).

Vertisol was found near the Acaraú River delta at a lower elevation (7 m) than the Planosol site. The profile was formed from sediments deposited by an intermittent creek. The Vertisol clay sample (Figure 2c) had a similar pattern to that of Planosol, although clay activity was lower in Vertisol than in Planosol. The XRD of Vertisol showed a higher-intensity peak at 1.8 nm (Mg + glycol solvation) than that of Planosol, and the clay content was higher in Vertisol (Table 3). Smectite is commonly the major mineral in Vertisols, with kaolinite being of secondary importance. In contrast, kaolinite has been reported to be abundant in some Vertisols. In addition, several non-expanding clay minerals such as kaolinite and vermiculites are associated with Vertisols and their vertic properties (Pal et al., 2012).

The micromorphological features of Vertisol were similar to those of Fluvisol, with similar coarse grains and microstructure, suggesting that the profile was more related to a sedimentary environment than to the pedological processes itself. In contrast, Vertisol showed strong aggregation, as seen in micromorphological slides and field analyses, associated with high clay content and 2:1 phyllosilicate mineralogy. Fluvisol and Vertisol shared a common sedimentary origin, but Fluvisol had a lower level of pedogenic development, partially because of its position on the landscape (Pal et al., 2012). The proximity of Vertisol to the coast was responsible for particular features, such as high salinity (revealed by ESP) and precipitation of salt crystals on aggregate surfaces. The high Na⁺ concentration (accumulation of exchangeable Na⁺) is evidence of sodification (Buol et al., 2011).

Seasonal cracking of soil profiles leads to pedoturbation (Buol et al., 2011), which results in heterogeneous zones along the matrix background. Pore hypocoatings are likely derived from iron and manganese precipitates that become mobile when soil is saturated (Lindbo et al., 2010). Iron nodules with altered micromorphological characteristics were also observed, suggesting *ex situ* genesis and in-progress destruction.

Solonchak was located even closer to the mouth of the Acaraú River, at an elevation of 5 m (fluvio-marine plain of the Acaraú River). Pedogenesis was strongly influenced by the shallow water table (about 1 m deep) and salt abundance, resulting in high EC values compared with other profiles. The Solonchak sample (Figure 2d) comprised both 1:1 and 2:1 phyllosilicates. Different from the observed in other profiles, the broad band at 1.3 nm collapsed to 1.0 nm with K saturation at 300 °C. The peak near 1.6 nm was maintained even after Mg and Mg + glycol solvation, indicating an interstratified material. Andrade et al. (2014) investigated the same area near the Acaraú River and identified a predominance of illite instead of kaolinite and a mixed-layer mineral, probably a kaolinite/smectite or an interstratified smectite/illite.

As also observed for Vertisol, the high ESP processes of Solonchak (Table 4) were an indication of sodification associated with salinization processes. A constantly humid environment prevents aggregate and microaggregate development, resulting in low porosity. According to Nascimento et al. (2015), low porosity may be related to the dense filling of voids by fine materials. Hypocoating occurred in pores formed by grass root activity and were identified in the field as small mottles, more common in superficial horizons. The profile was located in an *apicum* area, where the frequency of tidal flooding led to hydromorphism and salt-related morphological features (Albuquerque et al., 2014a). Lithological discontinuity was suggested in this profile because of its erratic distribution of particle size and TOC. Such findings agree with the general hypothesis that Solonchak was formed by fluvio-marine-eolian sediments (Meireles et al., 2007; Bliedtner et al., 2018). The mineralogy of the Solonchak clay fraction is similar to that of other mangrove soils, comprising kaolinite, illite, and smectite (Ferreira et al., 2010; Andrade et al., 2018).

CONCLUSIONS

The main driving factor of the pedogenesis of the studied soils was their position along the lower course of the Acaraú River, which resulted in different sedimentary environments and hydrologic dynamics. Their contrasting pedogenesis was reflected in their morphological, chemical, and physical properties and supported by the alluvial nature of the parent material, as revealed by micromorphological examination.

The results provided evidence of the following pedogenic processes: i) eluviation and illuviation of clay, although only incipient in Planosol; ii) gleying, particularly in Solonchak; iii) pedoturbation in Vertisol; and iv) salinization and sodification, particularly in near-coast profiles located close to the coast (Vertisol and Solonchak).

ACKNOWLEDGEMENTS

This study was financed in part by the Coordenação de Aperfeiçoamento de Pessoal de Nível Superior - Brasil (CAPES) - PROCAD, Finance Code 064/2010.

AUTHOR CONTRIBUTIONS

Conceptualization:  Rafael Cipriano-Silva (equal),  Gustavo Souza Valladares (equal), and  Marcos Gervasio Pereira (equal).

Methodology:  Rafael Cipriano-Silva (lead),  Gustavo Souza Valladares (lead), and  Carlos Roberto Pinheiro Junior (supporting).

Validation:  Rafael Cipriano-Silva (equal),  Gustavo Souza Valladares (equal),  Antônio Carlos de Azevedo (equal),  Lúcia Helena Cunha dos Anjos (equal),  Marcos Gervasio Pereira (equal), and  Carlos Roberto Pinheiro Junior (equal).

Formal analysis:  Rafael Cipriano-Silva (lead) and  Antônio Carlos de Azevedo (supporting).

Investigation:  Rafael Cipriano-Silva (equal) and  Gustavo Souza Valladares (equal).

Resources:  Gustavo Souza Valladares (equal),  Antônio Carlos de Azevedo (equal),  Lúcia Helena Cunha dos Anjos (equal), and  Marcos Gervasio Pereira (equal).

Data curation:  Rafael Cipriano-Silva (lead).

Writing - original draft:  Rafael Cipriano-Silva (equal),  Gustavo Souza Valladares (equal),  Lúcia Helena Cunha dos Anjos (equal), and  Marcos Gervasio Pereira (equal).

Writing - review and editing:  Rafael Cipriano-Silva (equal),  Gustavo Souza Valladares (equal),  Antônio Carlos de Azevedo (equal),  Lúcia Helena Cunha dos Anjos (equal),  Marcos Gervasio Pereira (equal), and  Carlos Roberto Pinheiro Junior (equal).

Visualization:  Rafael Cipriano-Silva (equal),  Gustavo Souza Valladares (equal), and  Marcos Gervasio Pereira (equal).

Supervision:  Gustavo Souza Valladares (lead),  Antônio Carlos de Azevedo (supporting),  Lúcia Helena Cunha dos Anjos (supporting), and  Marcos Gervasio Pereira (supporting).

Project administration:  Gustavo Souza Valladares (lead),  Lúcia Helena Cunha dos Anjos (supporting), and  Marcos Gervasio Pereira (supporting).

Funding acquisition:  Gustavo Souza Valladares (lead),  Lúcia Helena Cunha dos Anjos (supporting), and  Marcos Gervasio Pereira (supporting).

REFERENCES

- Albuquerque AGBM, Ferreira TO, Cabral RL, Nóbrega GN, Romero RE, Meireles AJA, Otero XL. Hypersaline tidal flats (*apicum* ecosystems): the weak link in the tropical wetlands chain. *Environ Rev.* 2014b;22:99-109. <https://doi.org/10.1139/er-2013-0026>
- Albuquerque AGBM, Ferreira TO, Nóbrega GN, Romero RE, Souza Júnior VS, Meireles AJA, Otero XL. Soil genesis on hypersaline tidal flats (*apicum* ecosystem) in a tropical semi-arid estuary (Ceará, Brazil). *Soil Res.* 2014a;52:140-54. <https://doi.org/10.1071/SR13179>
- Alvares CA, Stape JL, Sentelhas PC, Moraes G, Leonardo J, Sparovek G. Köppen's climate classification map for Brazil. *Meteorol Z.* 2013;22:711-28. <https://doi.org/10.1127/0941-2948/2013/0507>
- Andrade GRP, Azevedo AC, Cuadros J, Souza VS, Furquim SAC, Kiyohara PK, Vidal-Torrado P. Transformation of kaolinite into smectite and iron-illite in Brazilian mangrove soils. *Soil Sci Soc Am J.* 2014;78:655-72. <https://doi.org/10.2136/sssaj2013.09.0381>
- Andrade GRP, Cuadros J, Partiti CSM, Cohen R, Vidal-Torrado P. Sequential mineral transformation from kaolinite to Fe-illite in two Brazilian mangrove soils. *Geoderma.* 2018;309:84-99. <https://doi.org/10.1016/j.geoderma.2017.08.042>
- Barnhisel RI, Bertsch PM. Chlorites and hydroxy-interlayered vermiculite and smectite. In: Dixon JB, Weed SB, editors. *Minerals in soil environments*. Madison: Soil Science Society of America; 1989. p. 729-88.

- Bétard F, Caner L, Gunnell Y, Bourgeon G. Illite neoformation in plagioclase during weathering: Evidence from semi-arid Northeast Brazil. *Geoderma*. 2009;152:53-62. <https://doi.org/10.1016/j.geoderma.2009.05.016>
- Bullock P, Fedoroff N, Jongerius A, Stoops G, Tursina T. Handbook for soil thin section description. Albrighton: Waine Research Publication; 1985.
- Buol SW, Southard RJ, Graham RC, McDaniel PA. Soil genesis and classification. 6. ed. Chichester: John Wiley & Sons; 2011.
- Bliedtner M, Zech R, Kühn P, Schneider B, Zielhofer C, von Suchodoletz H. The potential of leaf wax biomarkers from fluvial soil-sediment sequences for paleovegetation reconstructions-Upper Alazani River, central southern Greater Caucasus (Georgia). *Quaternary Sci Rev*. 2018;196:62-79. <https://doi.org/10.1016/j.quascirev.2018.07.029>
- Cabral LJRS, Valladares GS, Pereira MG, Pinheiro Júnior CR, Lima AM, Frota JCO, Amorim JVA. Classificação dos solos da Planície do Delta do Parnaíba, PI. *Rev Bras Geog Fis*. 2019;12:1466-83.
- Castro SS, Cooper M. Fundamentos de micromorfologia de Solos. Viçosa, MG: Sociedade Brasileira de Ciência do Solo; 2019.
- Celarino ALS, Ladeira FSB. How fast are soil-forming processes in Quaternary sediments of a tropical floodplain? A case study in southeast Brazil. *Catena*. 2017;156:263-80. <https://doi.org/10.1016/j.catena.2017.04.002>
- Damm B, Hagedorn J. Holocene floodplain formation in the southern Cape region, South Africa. *Geomorphology*. 2010;122:213-22. <https://doi.org/10.1016/j.geomorph.2009.06.025>
- Diniz SF, Kelting FMS, Rueda JBJ. Análise fisiográfica solo/paisagem do Rio Acaraú-CE. *Revista Anpege*. 2011;7:143-54. <https://doi.org/10.5418/RA2011.0707.0010>
- Diniz SF, Moreira CA, Corradini FA. Susceptibilidade erosiva do baixo curso do rio Acaraú-CE. *Geociências*. 2008;27:355-67.
- Eze PN, Knight J, Evans M. Tracing recent environmental changes and pedogenesis using geochemistry and micromorphology of alluvial soils, Sabie-Sand River Basin, South Africa. *Geomorphology*. 2016;268:312-21. <https://doi.org/10.1016/j.geomorph.2016.06.023>
- Ferreira TO, Otero XL, Souza Junior VS, Vidal-Torrado P, Macías F, Firme LP. Spatial patterns of soil attributes and components in a mangrove system in Southeast Brazil (São Paulo). *J Soils Sediments*. 2010;10:995-1006. <https://doi.org/10.1007/s11368-010-0224-4>
- Gama AF, Cavalcante RM, Duaví WC, Silva VPA, Nascimento RF. Occurrence, distribution, and fate of pesticides in an intensive farming region in the Brazilian semi-arid tropics (Jaguaribe River, Ceará). *J Soils Sediments*. 2017;17:1160-9. <https://doi.org/10.1007/s11368-016-1597-9>
- IUSS Working Group WRB. World reference base for soil resources 2014, update 2015: International soil classification system for naming soils and creating legends for soil maps. Rome: Food and Agriculture Organization of the United Nations; 2015. (World Soil Resources Reports, 106).
- Jacomine PKT, Almeida JC, Medeiros LAR. Levantamento exploratório - reconhecimento de solos do estado do Ceará. Recife: Divisão de pesquisa pedológica - DNPEA; 1973. (Boletim técnico, 28).
- Kovda I, Mermut A. Vertic features. In: Stoops G, Marcelino V, Mees F, editors. Interpretation of micromorphological features of soils and regoliths. Amsterdam: Elsevier; 2010. p. 109-27.
- Lindbo DL, Stolt MH, Vepraskas MJ. Redoximorphic features. In: Stoops G, Marcelino V, Mees F, editors. Interpretation of micromorphological features of soils and regoliths. Amsterdam: Elsevier; 2010. p. 129-47.
- Meireles AJA, Cassola RS, Tupinambá SV, Queiroz LS. Environmental impacts promoted by shrimp farm on the coast Ceará, northeastern Brazil. *Mercator*. 2007;6:83-106. <https://doi.org/10.1016/j.marpolbul.2006.07.006>
- Melo VF, Fontes MPF, Novais RF, Singh B, Schaefer CEGR. Características dos óxidos de ferro e de alumínio de diferentes classes de solos. *Rev Bras Cien Solo*. 2001;25:19-32. <https://doi.org/10.1590/S0100-06832001000100003>

- Mota LHSO, Gomes AS, Valladares GS, Magalhães RMF, Leite HMF, Silva TA. Risco de salinização das terras do baixo Acaraú (CE). *Rev Bras Cienc Solo*. 2012;36:1203-10. <https://doi.org/10.1590/S0100-06832012000400014>
- Mota LHSO, Valladares GS. Vulnerabilidade à degradação dos solos da Bacia do Acaraú, Ceará. *Rev Cienc Agron*. 2011;42:39-50. <https://doi.org/10.1590/S1806-66902011000100006>
- Mota LHSO, Valladares GS, Leite HMF, Gomes AS, Magalhães RMF, Silva TA. Análise multitemporal do uso e cobertura das terras da Região do Baixo Acaraú - CE. *Geociências*. 2013;32:379-96.
- Nascimento AF, Furquim SAC, Graham RC, Beirigo RM, Oliveira Junior JC, Couto EG, Vidal-Torrado P. Pedogenesis in a Pleistocene fluvial system of the Northern Pantanal - Brazil. *Geoderma*. 2015;255-256:58-72. <https://doi.org/10.1016/j.geoderma.2015.04.025>
- Nascimento FR, Cunha SB, Rosa MF. Classes de solos e unidades morfo-pedológicas na bacia hidrográfica do Rio Acaraú, Ceará. In: VI Simpósio Nacional de Geomorfologia/Regional Reference on Geomorphology, Goiânia. Goiânia: Sinageo; 2006. Available from: <http://lsie.unb.br/ugb/sinageo/6/1/016.pdf>.
- Pal DK, Wani SP, Sahrawat KL. Vertisols of tropical Indian environments: Pedology and edaphology (Review). *Geoderma*. 2012;189-190:28-49. <https://doi.org/10.1016/j.geoderma.2012.04.021>
- Palmer A. Inceptisols. In: Elias S, editor. Reference module in earth systems and environmental sciences. Amsterdam: Elsevier; 2013. p. 248-54.
- Parahyba RBV, Santos MC, Rolim Neto FC, Jacomine PKT. Pedogênese de Planossolos em topossequência do agreste pernambucano. *Rev Bras Cienc Solo*. 2010;34:1991-2000. <https://doi.org/10.1590/S0100-06832010000600023>
- Pinheiro Junior CR, Pereira MG, Fontana A, Luz LRQPD, Corrêa Neto TDA. Pedogenesis in a topo-climosequence in the Agreste region of Pernambuco. *Rev Cienc Agron*. 2019;50:177-87. <https://doi.org/10.5935/1806-6690.20190021>
- Santos HG, Jacomine PKT, Anjos LHC, Oliveira VA, Lumbrreras JF, Coelho MR, Almeida JA, Araújo Filho JC, Oliveira JB, Cunha TJF. Sistema brasileiro de classificação de solos. 5. ed. rev. ampl. Brasília, DF: Embrapa; 2018.
- Santos RD, Lemos RC, Santos HG, Ker JC, Anjos LHC. Manual de descrição e coleta de solo no campo. 6. ed. Viçosa, MG: Sociedade Brasileira de Ciência do Solo; 2015.
- Sartor LR, Azevedo AC. Pilarização de argilas e perspectivas de aplicação e de pesquisa agrônômica e ambiental. *Rev Cienc Rural*. 2014;44:1541-8. <https://doi.org/10.1590/0103-8478cr20131536>
- Skorupa ALA, Silva SHG, Poggere GC, Tassinari D, Pinto LC, Zinn YL, Curi N. Similar soils but different soil-forming factors: converging evolution of Inceptisols in Brazil. *Pedosphere*. 2017;27:747-57. [https://doi.org/10.1016/S1002-0160\(17\)60443-0](https://doi.org/10.1016/S1002-0160(17)60443-0)
- Sobrinho JF. A compartimentação geomorfológica do Vale do Acaraú: distribuição das águas e pequeno agricultor. *Mercator*. 2006;10:91-110.
- Teixeira PC, Donagemma GK, Fontana A, Teixeira WG. Manual de métodos de análise de solo. 3. ed. rev e ampl. Brasília, DF: Embrapa; 2017.
- van Ranst E, Dumon M, Tolossa AR, Cornelis JT, Stoops G, Vandenberghe RE, Deckers J. Revisiting ferrolysis processes in the formation of Planosols for rationalizing the soils with stagnic properties in WRB. *Geoderma*. 2011;163:265-74. <https://doi.org/10.1016/j.geoderma.2011.05.002>